De-coupling Anomalous Fluid and Lithology Resistivity Effects by Using the Complete Seismic Wavefield

A.J. McKay* (PGS Geophysical AS), G. Rønholt (PGS Geophysical AS), T. Tshering (PGS Geophysical AS) & S. Naumann (PGS Geophysical AS)

SUMMARY

We present a workflow that enables identification and characterization of leads and prospects by combining all recorded wavefields from dual-sensor streamer seismic data and the sub-surface resistivity derived from Towed Streamer EM data. Deep tow, dual-sensor seismic acquisition does not only provide low-frequency rich, high signal-to-noise data, that is the foundation for high-resolution broadband imaging, but also serves as the ideal input for refraction based velocity estimation through full waveform inversion (FWI). In shallow water environments conventional 3D seismic imaging often struggles to provide accurate, high resolution imaging of the near surface mainly due to the lack of near offsets (angles) in typical 3D marine seismic data. However, dual-sensor seismic data also provide separated (up- and down-going) wavefields that we use to construct images and image gathers that span a complete range of incidence angles enabling amplitude versus angle (AVA) analysis to be carried out. We show that combining high resolution seismic velocity and resistivity models enables identification and isolation of background trends, and the correlation between anomalously high resistivity and low velocity zones to be investigated. This is a potentially useful precursory/complimentary activity to the robust AVA driven prospect and lead analysis enabled by the dual-sensor seismic data.

Introduction

A total of 10,200 km^2 of seismic data covering the Northern area of the former disputed zone between Norway and Russia was acquired in the so-called Barents Sea South East (BSSE) during the summers of 2014 and 2015. An exacting weather window and aggressive deadlines meant that acquisition efficiency was the priority. Consequently, the vessel deployed 12 dual-sensor streamers, 7km long and 75m apart and towed at 25m depth. The relatively small streamer separation (compared to the more common 100m for exploration surveys) was intended to improve illumination of shallow targets as one of the main plays in the BSSE is particularly shallow, and there are numerous high amplitude events and/or flat spots (see Figure 1 for example). Nevertheless, acquiring 3D towed streamer seismic data in shallow waters always involves a compromise between efficiency and near-surface sampling. However, by utilizing all components of the wavefield in seismic imaging, including the up- and down-going wavefields, the angle illumination of the near surface can be improved significantly.
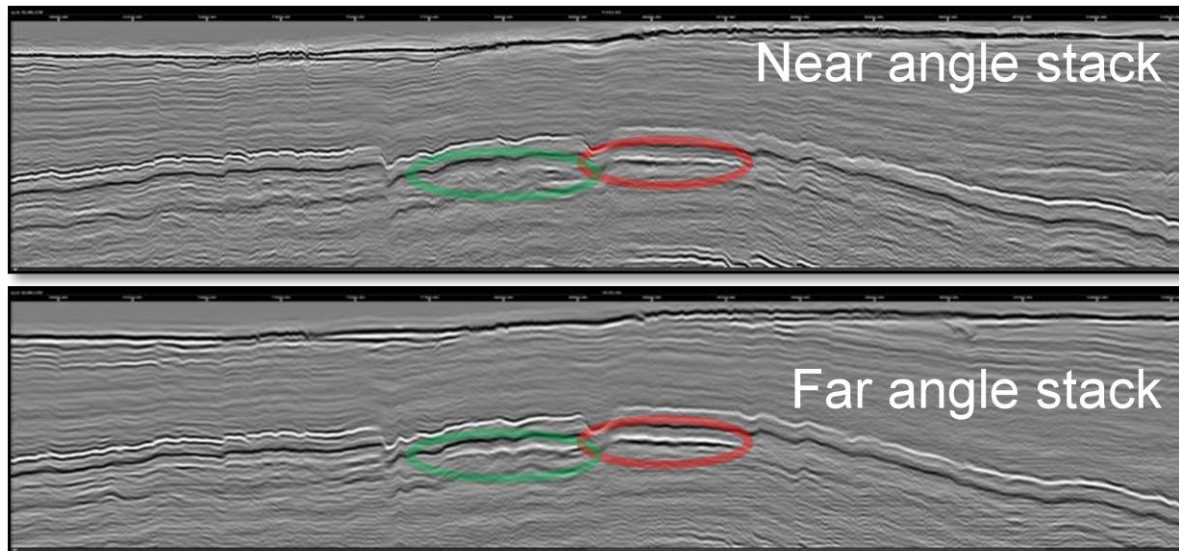
Figure 1 *Example image showing shallow, soft bright spots and AVA anomalies (red and green circles).*

By employing a Towed Streamer EM system it has now become possible to acquire Controlled Source Electromagnetic (CSEM) to determine the sub-surface resistivity very efficiently. Indeed, good quality Towed Streamer EM data were acquired over the same survey area as the streamer seismic acquisition, thus opening the door for a combination of seismic attributes and sub-surface resistivity measurements.

Seismic data are known to be most sensitive to a change in hydrocarbon saturation at the low end of saturation (e.g. < 50%). Therefore, the AVA response illustrated in Figure 1, even if due solely to the presence of hydrocarbons, would be similar regardless of whether the saturation is relatively low or high. CSEM data are most sensitive to a change in saturation when saturation is relatively high (e.g. > 50%). However, as is well known, sub-surface resistivity varies in response to both fluid and lithology changes e.g. the resistivity of say carbonates can be greater than that of a hydrocarbon charged sand, but the acoustic properties of the carbonate should be inconsistent with a sand charged with oil or gas. Thus, by combining both acoustic and electromagnetic attributes it should be possible to discriminate between lithology and fluid effects, and de-risk saturation levels, by exploiting the complimentary information and sensitivity to fluid and lithology provided by the two different data types.

This paper has three main parts. First, we review briefly the main elements of the seismic imaging workflow that both improves the near surface imaging and produces a high resolution velocity model. Second, we review briefly the inversion methodology used to determine the sub-surface resistivity from the Towed Streamer Data. Finally, we present the joint analysis of the high resolution velocity and sub-surface resistivity models.

Complete Wavefield Imaging Methodology

The Complete Wavefield Imaging (CWI) workflow is made up of three main elements: wavelet shift tomography, full waveform inversion (FWI) and separated wavefield imaging (SWIM). The key to producing highly accurate velocity models and images is how the three imaging techniques are combined into a workflow that mitigates any weakness that might exist in any one method alone (see for example Rønholt et al., 2014).

Leveraging the good low frequency data recorded by dual-sensor towed streamer data, FWI produces high-resolution velocity model updates from the seafloor down to depths where the refracted energy diminishes.

In contrast to imaging with primary reflections separated wavefield imaging (Whitmore et al., 2010) uses sea-surface reflections, effectively turning each receiver into a virtual source, hence significantly improving the source sampling. The improved illumination provided by the additional virtual sources leads to improved imaging of the shallow sub-surface (Lu et al., 2014) and well sampled angle gathers.

Towed Streamer EM Inversion Methodology

We use unconstrained inversion of the Towed Streamer EM data to determine the sub-surface resistivity as we aim to extract the maximum possible amount of information from the EM data without constraining the model. Previous case studies show that the data-density of Towed Streamer EM data enables the reliable and accurate determination of sub-surface resistivity using unconstrained inversion; see for example McKay et al. (2015). In any case, in a frontier exploration setting such as the BSSE then geological knowledge is limited: there are no wells and little a-priori information to provide model parameter constraints. Regardless, we need to ensure that the resistivity model is an independent source of information: we wish to investigate the correlation between the acoustic and electromagnetic parameters, not induce correlation.

Therefore, the Towed Streamer EM data were inverted in 3D using the unconstrained anisotropic inversion methodology outlined by Zhdanov et al. (2014). No seismic data and/or resistivity parameter constraints are used to restrict the determination of the vertical and horizontal resistivity, or anisotropy. A key feature of the 3D inversion is the footprint methodology where the data are inverted all at once, but the modelling domain is decomposed into numerous sub-domains based on sensitivity measures. This decomposition enables large-scale and efficient inversion, and a single consistent model. In general the inversion model quality is good with a relative data misfit of $< 3\%$.

Joint Interpretation

One practical advantage of undertaking the CWI workflow is that both the seismic and EM volumes are in the depth domain. This makes the initial data integration relatively trivial although we do have to be mindful of the differing resolution of the acoustic and electromagnetic properties. Nevertheless, the first step in the workflow is to simply overlay seismic and EM volumes to examine the degree of conformance between say the main stratigraphic boundaries and resistivity units. However, for brevity we do not show an example here.
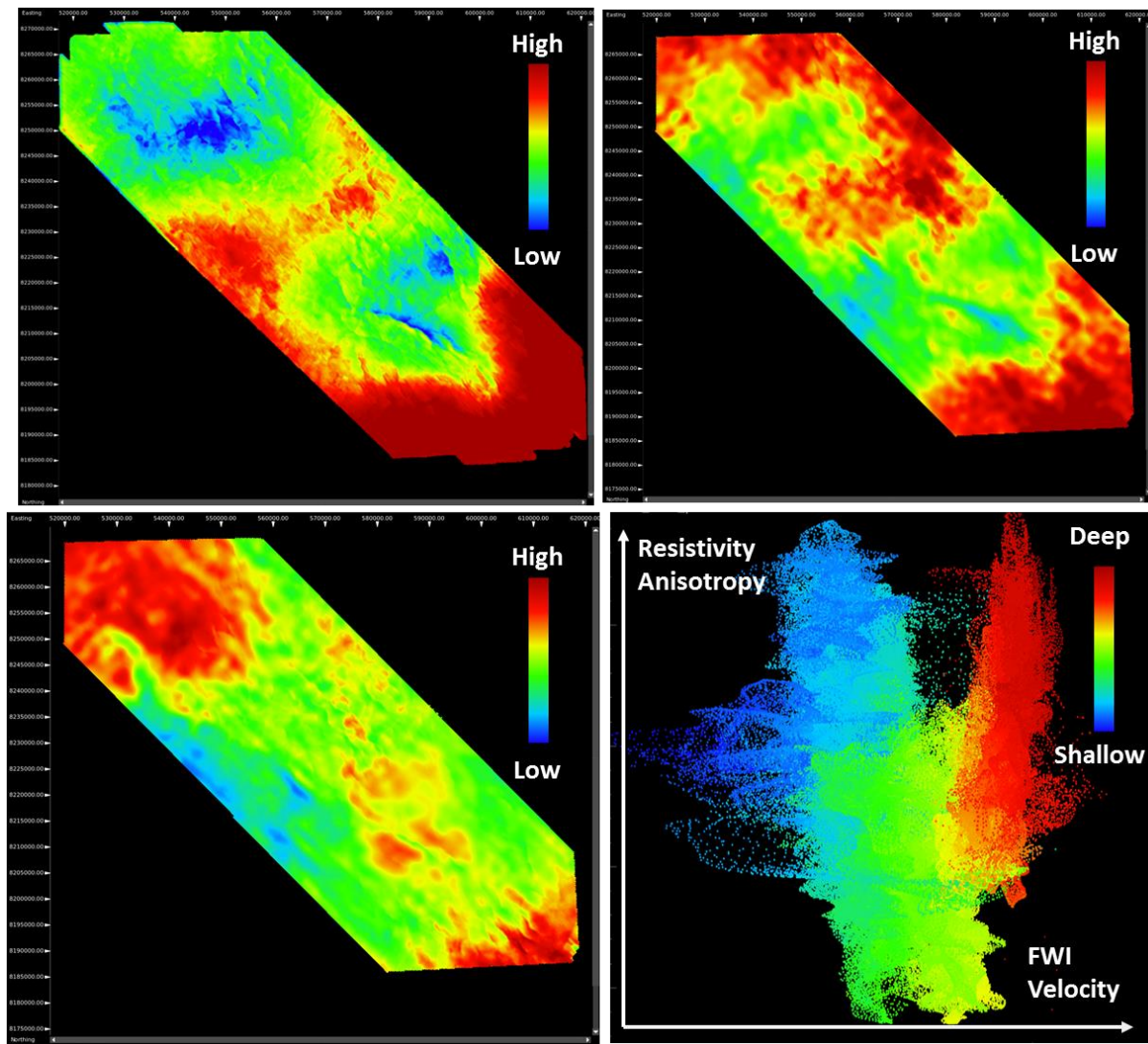
Figure 2 *Average attributes extracted over a 200m interval of interest: FWI Velocity (top left), Vertical Resistivity (top right) and Resistivity Anisotropy (bottom left). Cross plot of resistivity anisotropy vs. FWI velocity over the same 200 m interval: the colour coding indicates depth and spans a range of about 500 m.*

The second step is to compare the high resolution velocity and sub-surface resistivity models. To enable comparison of the lateral variations in velocity and resistivity on approximately the same scale we extracted the average velocity and resistivity over a given depth interval. In Figure 2 the average FWI velocity, unconstrained vertical resistivity and anisotropy, extracted over a 200 m interval below an interpreted horizon, are shown. First of all, the FWI velocities show clearly that there are two obvious low velocity structures: these correspond to the two main structural highs in the area. Closer examination of the FWI velocities reveals that many of the low velocity features correspond very well with the structural highs and other acoustic features such as potential flat spots and amplitude brightening. Indeed, detailed reservoir characterisation analysis (not shown for brevity) indicates that the low velocity zones correlate extremely well with other attributes such as low acoustic impedance and low Vp/Vs (derived from AVA inversion of pre-stack data from separated wavefield imaging). However, the same depth interval is relatively resistive off-structure and more conductive on-structure, which at first may be disappointing from the exploration perspective since in general we are expecting high resistivity associated with hydrocarbon charged sands. Nevertheless, the gross lateral trends in resistivity and velocity are comparable which suggests that the same mechanism (e.g. depth

trend or change of facies) is driving the variation of both, while the background trend in resistivity may be masking more subtle variations of interest.

Consequently, the third step is to estimate the background trend in sub-surface resistivity, which could be attempted in a number of ways. We determined the average background vertical resistivity over the same depth interval by predicting it from the horizontal resistivity and an estimate of regional anisotropy: the predicted background resistivity was then subtracted to determine an anomalous vertical resistivity. We found that in this case the anomalous vertical resistivity is very similar to the anisotropy shown in Figure 2: with the anomalous areas of resistivity confined mainly to the structural highs.

As the final step we examined the relation between the various attributes via cross-plots. In Figure 2 a cross-plot of resistivity anisotropy and FWI velocity is shown with the colour coding denoting interval depth (blue shallow; red deep). Clearly, there is some correspondence between high anisotropy (and therefore potentially anomalous resistivity), low velocity and the shallowest depths (structural highs).

Summary and Conclusions

A high resolution velocity model is but one of the products of the CWI workflow enabled by broadband dual-sensor seismic data. Combining the high resolution velocity model with the unconstrained sub-surface resistivity model enables a relatively quick and easy integration of the acoustic and electromagnetic properties. The correlation between the variation in velocity and resistivity implies that if we can understand the background trend in at least one of the properties then we may be able to exploit the correlation to define a robust background trend and thus define anomalous areas of interest e.g. anomalously high resistivity associated with low velocity thereby enabling improved ranking and/or de-risking of prospects in a frontier exploration setting.

Acknowledgments

References

Lu, S., D. Whitmore, A. Valenciano, and N. Chemingui [2014] Enhanced subsurface Illumination from separated wavefield imaging. *First Break*, **32**(12), 87-92.

McKay, A., Mattsson, J. and Du, Z. [2015] Towed Streamer EM – reliable recovery of sub-surface resistivity. *First Break,* **33**, 75-85.

Rønholt, G., Lie, J. E., Korsmo, O., Danielsen, B., Brandsberg-Dahl, S., Brown, S., Chemingui, N., Valenciano Mavilio, A., and Whitmore, D. [2014] Broadband velocity model building and imaging using reflections, refractions and multiples from dual-sensor streamer data, *76th EAGE Conference & Exhibition.*

Zhdanov, M.S., Endo, M., Yoon, D., Cuma, M., Mattsson, J. and Midgley, J., [2014] Anisotropic 3D inversion of towed streamer electromagnetic data: Case study from the Troll West Oil Province. *Interpretation*, **2**(3) (August 2014); p. SH01–SH17.

Whitmore, N.D., Valenciano, A.A., Söllner, W. and Lu, S. [2010] Imaging of primaries and multiples using a dual-sensor towed streamer. *80th SEG Meeting*, Expanded Abstracts, 3187-3192.